Burst firing of neurons in the thalamic reticular nucleus during locomotion

Vladimir Marlinski and Irina N. Beloozerova

J Neurophysiol 112:181-192, 2014. First published 16 April 2014; doi:10.1152/jn.00366.2013

Journal of Neurophysiology publishes original articles on the function of the nervous system. It is published 12 times a year (monthly) by the American Physiological Society, 9650 Rockville Pike, Bethesda MD 20814-3991. ISSN: 0022-3077, ESSN: 1522-1598. Visit our website at http://www.the-aps.org/.

J Neurophysiol 112: 181–192, 2014.
First published April 16, 2014; doi:10.1152/jn.00366.2013.

Burst firing of neurons in the thalamic reticular nucleus during locomotion

Vladimir Marlinski and Irina N. Beloozerova
Division of Neurobiology, Barrow Neurological Institute, Phoenix, Arizona

Submitted 20 May 2013; accepted in final form 14 April 2014

Marlinski V, Beloozerova IN. Burst firing of neurons in the thalamic reticular nucleus during locomotion. *J Neurophysiol* 112: 181–192, 2014. First published April 16, 2014; doi:10.1152/jn.00366.2013.—This study examined the burst firing of neurons in the motor sector of the thalamic reticular nucleus (RE) of the cat. These neurons are inhibitory cells that project to the motor thalamus. The firing activity of RE neurons was studied during four behaviors: sleep, standing, walking on a flat surface, and accurate stepping on crosspieces of a horizontal ladder. Extracellularly recorded firing activity was analyzed in 58 neurons that were identified according to their receptive fields on the contralateral forelimb. All neurons generated bursts of spikes during sleep, half generated bursts of spikes during standing, and one-third generated bursts of spikes during walking. The majority of bursts were sequences of spikes with an exponential buildup of the firing rate followed by exponential decay with time constants in the range of 10–30 ms. We termed them "full-scale" bursts. All neurons also generated "atypical" bursts, in which the buildup of the firing rate deviated from the characteristic order. Burst firing was most likely to occur in neurons with receptive fields on the distal forelimb and least likely in neurons related to the proximal limb. Full-scale bursts were more frequent than atypical bursts during unconstrained walking on the flat surface. Bursts of both types occurred with similar probability during accurate stepping on the horizontal ladder, a task that requires forebrain control of locomotion. We suggest that transformations of the temporal pattern of bursts in the inhibitory RE neurons facilitate the tuning of thalamo-cortical signals to the complexity of ongoing locomotor tasks.

cat; burst of spikes; thalamus; motor cortex; walking

THE THALAMIC RETICULAR NUCLEUS (RE) surrounding the anterior, lateral, and ventral aspects of the dorsal thalamus is formed by a layer of inhibitory GABAergic neurons that project to the relay nuclei of the dorsal thalamus (Arcelli et al. 1997; Govindaiah and Cox 2006; Houser et al. 1980; Lam and Sherman 2007; Liu et al. 1995; Pinault and Deschênes 1998; Scheibel and Scheibel 1966; Velayos et al. 1989; Yen et al. 1985). RE neurons receive their inputs primarily from the relay thalamic nuclei and layer VI of the cortex (Carman et al. 1964; Crabtree 1992; Lam and Sherman 2011; Liu et al. 2001; Rinvik 1968). Thalamic and cortical inputs of similar modality converge in distinct sectors of the RE related to motor, somatosensory, auditory, visual, and visceral modalities (Crabtree 1992; Guillery and Harting 2003; Jones 1975; Pinault 2004).

RE neurons have two modes of firing activity, tonic and bursting (Hartings et al. 2003; Lee et al. 2007; Marlinski et al. 2012b; Mukhametov et al. 1970; Steriade et al. 1986). The bursting mode reflects occasional activation of the transient Ca^{2+} current that produces a low-threshold spike, on top of which sodium spikes occur (Bal and McCormick 1993; Huguenard and Prince 1992). Bursts of spikes generated by RE neurons have a unique temporal structure that is characterized by an initial progressive increase in the discharge rate followed by a progressive decrease in the discharge rate, artfully depicted as accelerando-ritardando or accelerando-decelerando pattern (Contreras et al. 1993; Domich et al. 1986; Mulle et al. 1986). Typically, in neurons of the relay thalamic nuclei and the RE the bursts are seen during sleep; however, they occur in alert subjects as well (Domich et al. 1986; Fanselow et al. 2001; Guido and Weyand 1995; Marlinski et al. 2012b; Swadlow and Gusev 2001; Weyand et al. 2001). For example, according to Domich and colleagues (1986), in RE neurons of the cat, bursts occur at a rate of ~25 per minute during sleep and 4 per minute during quiet wakefulness. Bursts during wakefulness may be of particular importance for transmitting signals from reticular to relay thalamic neurons. In thalamocortical pathways, it was shown that bursts facilitate signal transmission, as the coding efficiency of bursts of spikes considerably exceeds that of tonic firing (Nicolelis and Fanselow 2002; Reinagel et al. 1999; Swadlow and Gusev 2001; Swadlow et al. 2005). If considered as unitary events, bursts may encode three times more information than tonic spikes (Reinagel et al. 1999).

We focused our study on the motor sector of the RE, which receives its inputs from the motor cortex and the ventrolateral nucleus of the thalamus (VL). We have recently reported that, during locomotion, the firing activity of the vast majority of neurons in the motor sector of the RE is modulated in the rhythm of strides and differs between walking on a flat surface and accurate stepping on crosspieces of a horizontal ladder (Marlinski et al. 2012b). We also found that the firing activity during walking may include bursts of spikes. It is noteworthy that, despite differences in the average discharge rate, the stride-related modulation of the firing rate, and the phase and duration of periods of elevated activity seen in most neurons during walking on the flat surface and on the ladder, the likelihood of burst occurrence was similar in these two tasks. Nevertheless, taking into account that the differences in the complexity of these locomotor tasks are associated with substantial differences in the firing activity of neurons in both the motor cortex and the VL (Marlinski et al. 2012a; Sirota et al., 2005; Stout and Beloozerova 2012), we expected to see some differences in the burst firing of RE neurons. We hypothesized that these differences could be found in the number of spikes composing the burst, the burst duration, or the temporal pattern of the firing during the burst. To test these hypotheses, we analyzed the structure of bursts in RE neurons during different behaviors of the cat.

We recorded extracellularly from neurons in the motor sector of the RE in cats during sleep, standing, and walking on the flat surface and on the horizontal ladder. We found that

Address for reprint requests and other correspondence: V. Marlinski, Div. of Neurobiology, Barrow Neurological Inst., 350 West Thomas Rd., Phoenix, AZ 85013 (e-mail: vladimir.marlinski@chw.edu).

these neurons generated three types of busts: full-scale bursts with an exponential buildup in the firing rate and two types of atypical bursts, altered bursts whose initial buildup deviated from the exponential order and short bursts that started with their maximal firing rate. We found that full-scale bursts were more frequent than atypical bursts during walking on the flat surface, whereas during walking on the ladder the atypical bursts occurred as often as the full-scale bursts. We propose that this difference of the burst structure in RE neurons reflects differences in their cortical and thalamic inputs during locomotor tasks that do or do not require thalamo-cortical control of stepping. We suggest that atypical bursts that start with the highest firing rate increase the efficiency of signal transmission from the RE to thalamic relay neurons during complex locomotor tasks.

A brief account of this study has been published in abstract form (Marlinski and Beloozerova 2013).

METHODS

Extracellular recordings from single RE neurons were obtained during chronic experiments in two adult cats. From the sample of neurons located in the forelimb representation of the motor sector of the RE, described in our previous report (Marlinski et al. 2012b), we selected cells that met two requirements: *1*) the quality of recording from these cells was good enough to guarantee an identification of each spike, and *2*) receptive fields of these cells were thoroughly tested. The methods of surgical preparation, recording technique, and histological procedures have been described in detail in a previous report (Marlinski et al. 2012b) and are briefly outlined here. The experimental protocol complied with National Institutes of Health guidelines for the care and use of animals in research and was approved by the Barrow Neurological Institute Animal Care and Use Committee.

Behavioral tasks. Recordings were obtained in cats during sleep, standing, walking on a flat surface, and walking along a horizontal ladder. Cats often fell asleep for 5–15 min while sitting on a comfortable pad in a "sphinx" posture with their head restrained. The sleeping state was identified based on the pattern of electroencephalographic signals recorded from electrodes in the motor cortex (Marlinski et al. 2012b). After sleep, cats were engaged in two locomotor tasks of different complexities: walking on a flat surface and accurate stepping on crosspieces of a horizontal ladder. Walking on a flat surface does not require vision and can be accomplished without forebrain control, whereas ladder locomotion relies on vision and necessitates participation of the thalamo-cortical network (Beloozerova and Sirota 1993, 2003; Chambers and Liu 1957; Friel et al. 2007; Liddell and Phillips 1944; Marigold and Patla 2008; Metz and Whishaw 2002; Rivers et al. 2011; Sherk and Fowler 2001; Trendelenburg 1911). The walking chamber was a rectangular enclosure with two connected parallel corridors (2.5 × 0.3 m each), one of which had a flat walking surface while the other contained a horizontal ladder. The centers of the 5-cm-wide crosspieces of the ladder were spaced 25 cm apart. The ladder was elevated above the chamber's floor by 6 cm. Except for the variability of stride lengths, which is much smaller during walking on the ladder, biomechanics and limb muscle activities in the cat during walking on the flat surface and along the horizontal ladder are fairly similar (Beloozerova et al. 2010).

While walking in the chamber, cats passed through the two corridors sequentially and repeatedly. After each round, food was dispensed into a feeding dish placed in one of the corners of the chamber. Cats were trained to stand in front of the feeding dish for 3–5 s before food was dispensed. During data analysis, 1 s in the middle of this period was considered as "standing."

Cats were accustomed to wear a light backpack with connectors and a sock with a small metal plate on the sole of the foot. During walking, the duration of swing and stance phases of the forelimb contralateral to the side of recording in the RE was monitored by measuring the electrical resistance between the plate and the floor. The cat's passage through the beginning and the end of each corridor was recorded with infrared photodiodes.

Surgical procedures. Surgery was performed under isoflurane anesthesia in aseptic conditions. A plastic circular base was attached to the skull with stainless steel screws (Prilutsky et al. 2005). The base was used for fixation of connectors, electrode microdrive, and preamplifier, as well as for holding the head of the cat during sleep and during search and identification of neurons. An arrangement of 8 (*cat 1*) or 19 (*cat 2*) 28-gauge hypodermic guide tubes was implanted vertically above the rostrolateral part of the left RE according to coordinates of the stereotaxic atlas of Reinozo-Suarez (1961). In addition, two similar guide tubes were implanted vertically above the left VL for insertion of stimulating electrodes. On the left side of the head, the dorsal surface of the rostral and lateral sigmoid gyri and the rostral part of the posterior sigmoid gyrus were exposed by removing ~1 cm^2 of bone and dura mater. The exposure was covered with a 1-mm-thick acrylic plate preperforated with holes of 0.36-mm diameter spaced 0.5 mm apart. The holes were filled with bone wax and allowed an insertion of stimulating electrodes in the motor cortex. Stimulating electrodes were made of Teflon-insulated platinum-iridium wire with a 140-μm outer diameter (A-M Systems). They were implanted into the VL and motor cortex representation of the distal and proximal forelimb after physiological mapping of these areas in the awake cat and were used to evoke responses in the RE.

Single-unit recording. Extracellular recordings were obtained with tungsten varnish-insulated microelectrodes (120-μm outer diameter, FHC) or platinum-tungsten quartz-insulated microelectrodes (40-μm outer diameter, Thomas Recording), both with 1- to 3-MΩ impedance at 1,000 Hz. A lightweight (2.5 g) manual single-axis micromanipulator, chronically mounted on the cat's head, was used to advance the microelectrode. Signals from the microelectrode were preamplified with a miniature preamplifier positioned on the cat's head and then further amplified and filtered (0.3- to 10-kHz band pass) with the CyberAmp 380 (Axon Instruments). After amplification, signals were digitized with a sampling frequency of 30 kHz (0.33-ms resolution) and recorded with a computerized data acquisition package (Power 1401/Spike2 System; Cambridge Electronic Design).

Identification of neurons and spike bursts. The main criterion for identification of RE neurons was characteristic bursts of spikes during sleep, within which the frequency of spikes first rises and then declines (Contreras et al. 1993; Domich et al. 1986; Marlinski et al. 2012b; Mukhametov et al., 1970; Steriade et al. 1986; Fig. 1, *A–C*). To determine whether recordings were obtained from the motor-related section of the RE, we tested responses of neurons to electrical stimulation of the motor cortex and VL with rectangular 0.2-ms pulses of 0.1–1.0 mA or 0.1–0.5 mA, respectively. To differentiate between ortho- and antidromic responses to the stimulation we used the collision test (Bishop et al. 1962; Fuller and Schlag 1976; see an example in Marlinski et al. 2012a). We considered neurons to be of the RE motor sector if they discharged bursts of spikes during sleep with the characteristic accelerando-decelerando pattern, responded transsynaptically to stimulation of the VL and motor cortex, and did not respond antidromically to stimulation of the motor cortex. Somatic receptive fields of neurons were examined in cats resting with their head restrained. Somatosensory stimulation was produced by stroking the fur and palpating the muscle bellies and tendons, as well as by passive joint movements.

To discriminate bursts from other irregularities in the firing activity of RE neurons, we set three initial temporal limits for the spike sequence similar to those of earlier studies: *1*) the first spike of the burst had to be preceded by silence lasting >50 ms; *2*) the first interspike interval within the burst had to be shorter than 20 ms; and

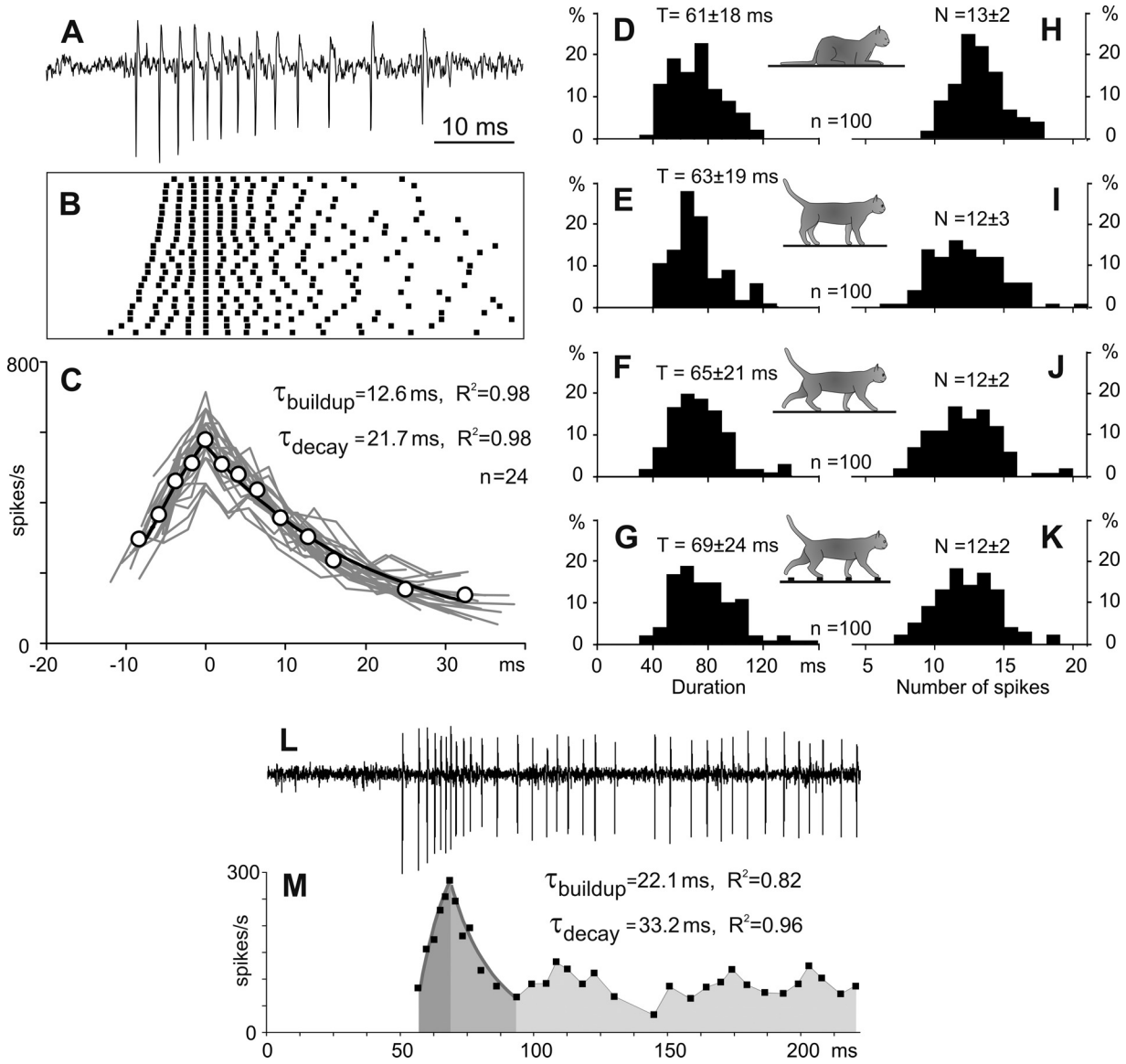

Fig. 1. The full-scale bursts of spikes in thalamic reticular nucleus (RE) neurons. *A*: representative full-scale burst recorded from a neuron during sleep. *B*: raster of spikes composing 24 spontaneous bursts generated by this neuron. *C*: instantaneous firing rates during each of these bursts (gray lines) and an average instantaneous firing rate (open circles). The buildup and decay of the averaged firing rate are fit with exponents (black lines), for which time constants (τ) and determination coefficients of fits (R^2) are indicated. *x*-Axes in *B* and *C* have the same timescale in milliseconds. *D–K*: histograms of duration (*D–G*) and number of spikes (*H–K*) of full-scale bursts recorded during sleep, standing, and walking on the flat surface and on the ladder, correspondingly (the data from randomly selected 100 bursts recorded during each behavior). *L* and *M*: a burst occurring at the beginning of an extended period of the firing activity. *L*: a representative record from a neuron. *M*: the firing rate of the neuron. Duration of the burst decay was estimated as a time interval with the highest accuracy of the fit. Dark and medium gray areas indicate periods of exponential buildup and decay of the burst, respectively. Time constants and determination coefficients of fits are indicated. The regular firing following the burst is highlighted with light gray.

3) during the burst, the peak firing rate had to exceed 200 spikes/s. In addition, we used two further criteria for distinction between burst and nonburst activity: the regularity in the rise and decline of the firing rate. First, only spike sequences within which a buildup of the firing rate was completed in an exponential fashion, or the firing rate was maximal from the beginning, were considered to be bursts. Second, only spike sequences within which the maximal firing rate was immediately followed by a decay that could be accurately approximated with an exponential function were considered to be bursts. This latter criterion was based on an assumption that the pattern of spike occurrences during the burst is defined by exponential changes in the membrane potential produced by T-Ca^{2+} current (Huguenard and Prince 1992). Periods of elevated activity that were composed of irregular changes in the firing rate were not identified as bursts.

Processing of neuronal activity. For the analysis of burst occurrences during different behaviors, bursts were considered as unitary events coinciding with the time of the first spike in the burst. The probability of burst occurrence during sleep and standing was evaluated as the number of bursts per second. The likelihood of bursts during walking was evaluated as the number of bursts per stride. To study neuronal activity during walking, data collected during two or three strides made in the middle of each corridor were used. During recordings from each individual neuron, only strides whose average duration during the two locomotor tasks differed by $<10\%$ were selected. The onset of the swing phase was taken as the beginning of the stride. The duration of each stride was divided into 20 equal bins. For each neuron, a histogram of spike activity in the stride cycle was generated for each walking task (see, e.g., Fig. 5, *F* and *G*, the shaded

area graphs). The histograms were smoothed by recalculating the value of each bin as follows: $F_n^{'} = 0.25 \times F_{n-1} + 0.5 \times F_n + 0.25 \times F_{n+1}$, where F_n is the original value of a bin. The first bin was considered to follow the last one; the last bin was considered to precede the first one. The difference between the maximal and minimal firing rate in the histogram was used to characterize the magnitude of modulation of the locomotion-related activity of the neuron. The neuron's average firing rate was calculated as a mean firing rate for all selected steps. Burst likelihood was calculated for each of the stride's bins, and the resulting histogram was smoothed in a way similar to that described above for simple spikes (see, e.g., Fig. 5, *F* and *G*, the red line graph). A two-tailed *t*-test was used to determine statistical differences; data are reported as means ± SD. The nonparametric χ^2-test was used for comparison of categorical data. Quantitative data analysis was done with Excel (Microsoft) and MATLAB (The MathWorks) custom-written programs.

Histology. At the termination of the experiments, cats were deeply anesthetized with pentobarbital sodium and reference electrolytic lesions were made in the areas of recording and stimulation. Cats were perfused with isotonic saline followed by a 3% paraformaldehyde solution. The positions of recording and stimulation electrodes in relation to the reference lesions were examined in 50-μm brain sections stained with cresyl violet. Details of the procedures are described in our previous report (Marlinski et al. 2012b).

RESULTS

This study included analysis of the firing activity of 58 neurons. Among them, 13 neurons responded to dorso- or ventroflexion of the wrist or pressure on the paw, and 2 of these neurons also had weak response to elbow movements; 7 neurons responded to flexion or extension of the elbow, and 3 of them had also weak response to shoulder movements; 18 neurons responded to movement in the shoulder, and among them 1 also had auxiliary response to elbow flexion; and 20 neurons did not respond to any somatosensory stimulation. The primary receptive field was used for the classification of neurons. From the firing activity of these 58 neurons a total of 2,454 bursts were identified and analyzed: 1,437 bursts were recorded during sleep, 670 bursts were obtained when cats were standing, 179 bursts were recorded during walking on the flat surface, and 168 bursts were recorded during walking along the ladder.

There are three types of bursts during sleep: full scale, altered, and short. The activity of all neurons was recorded when cats were sleeping for 5–15 min while sitting with their head restrained. During sleep, the firing activity of all neurons varied substantially. Periods of continuous regular firing, which represented the tonic mode, were mixed with periods of silence intermingled with sequences of spikes occurring at a high rate, which corresponded to the burst mode. The majority of bursts of spikes had a temporal structure consisting of a period of acceleration and a subsequent period of deceleration in the firing rate (Fig. 1, *A–C*). We classified these bursts as full-scale bursts. Within this basic temporal pattern, spike occurrence varied both between cells and within discharges of a single cell. This variability is illustrated in Fig. 1*B* as a raster of spikes that presents 24 bursts of a representative neuron. In this raster, the data are aligned on the spike that separated the acceleration and deceleration periods of the discharge within the burst and rank ordered according to the number of spikes that occurred before the maximal firing rate was reached (smaller at the top). In this example, the neuron generated 3–5 spikes before the peak firing in the burst was attained and then 5–10 more spikes afterwards. In the entire sample of bursts of all neurons, the acceleration period contained three to eight spikes. The duration of the first interspike interval within bursts varied considerably between 2 ms and 20 ms, with a mean of 3.4 ± 1.5 ms. Despite this variability, all bursts had an essential common feature: the firing rate changed in a fairly organized manner during both the acceleration and deceleration periods. During the activity buildup, an increase in the firing rate (FR) could be accurately approximated with an exponent: $FR = k \times [1 - \exp(-t/\tau)]$, where τ is the time constant, t is time, and k is the maximal firing rate. In the example shown in Fig. 1, *A–C*, the firing rate increased exponentially, with an average time constant of 12.6 ± 7.9 ms and a coefficient of determination $R^2 = 0.98$. At the peak, the instantaneous firing rate in this neuron could be as high as 600 spikes/s. The peak in the firing rate was followed by a period of discharge deceleration, during which the firing rate decayed exponentially: $FR = k \times \exp(-t/\tau)$, with a time constant of 21.7 ± 13.6 ms and $R^2 = 0.98$ (Fig. 1*C*). Time constants of the buildup and decay of the firing rate in individual neurons and between neurons varied in the range of 10–40 ms. Typically, the time constant of the firing deceleration was equal to or longer than the time constant of the firing acceleration. Occasionally, bursts were seen at the beginning of extended periods of the firing activity of the neuron when the deceleration period of the burst evolved into continuous regular firing (Fig. 1, *L* and *M*). In these cases, duration of the deceleration period could be determined by finding the time interval of the exponential fit yielding the best R^2 value (Fig. 1*M*). Thus as full-scale bursts we classified those bursts in which both the entire period of an increase in the discharge rate and the initial period of a decrease in the discharge rate could be accurately approximated with an exponential function. The characteristic full-scale bursts lasted 61 ± 18 ms and consisted of 13 ± 2 spikes, as evaluated in a representative group of 100 randomly selected bursts (Fig. 1, *D* and *H*).

The temporal structure of 5–40% bursts in each neuron was different from the full-scale pattern described above. This variability is illustrated in a fragment of a record from a representative neuron (Fig. 2). This fragment shows three bursts indicated on Fig. 2*A* with *indexes 1*, *2*, and *3*. These bursts are shown on an expanded timescale in Fig. 2, *B1–B3*, and the firing rates during bursts are shown in Fig. 2, *C1–C3* (in all panels, each of the bursts is identified with a corresponding numerical index). One of these bursts (*burst 1*) was a full-scale burst with a temporal structure similar to that shown in Fig. 1 (Fig. 2, *A1*, *B1*, and *C1*). During the other two bursts, the firing buildup deviated from the full-scale temporal structure. In *burst 2* (Fig. 2, *A2*, *B2*, and *C2*), the initially high firing rate decreased abruptly but then continued to increase exponentially with a time constant similar to that of the full-scale burst (Fig. 2*C2*). We called this type of bursts "altered." They could have one or two or occasionally three interspike intervals with high, but irregular, firing rates before an exponential buildup of the firing was established. Another burst (*burst 3*) lacked the activity acceleration period completely, and the firing started with the maximal rate (Fig. 2, *A3*, *B3*, and *C3*). We classified this type of burst as "short." We classified all bursts whose temporal structure deviated from the full-scale pattern as "atypical" bursts. Irrespective of the manner in which the firing rate reached its peak, the deceleration of the

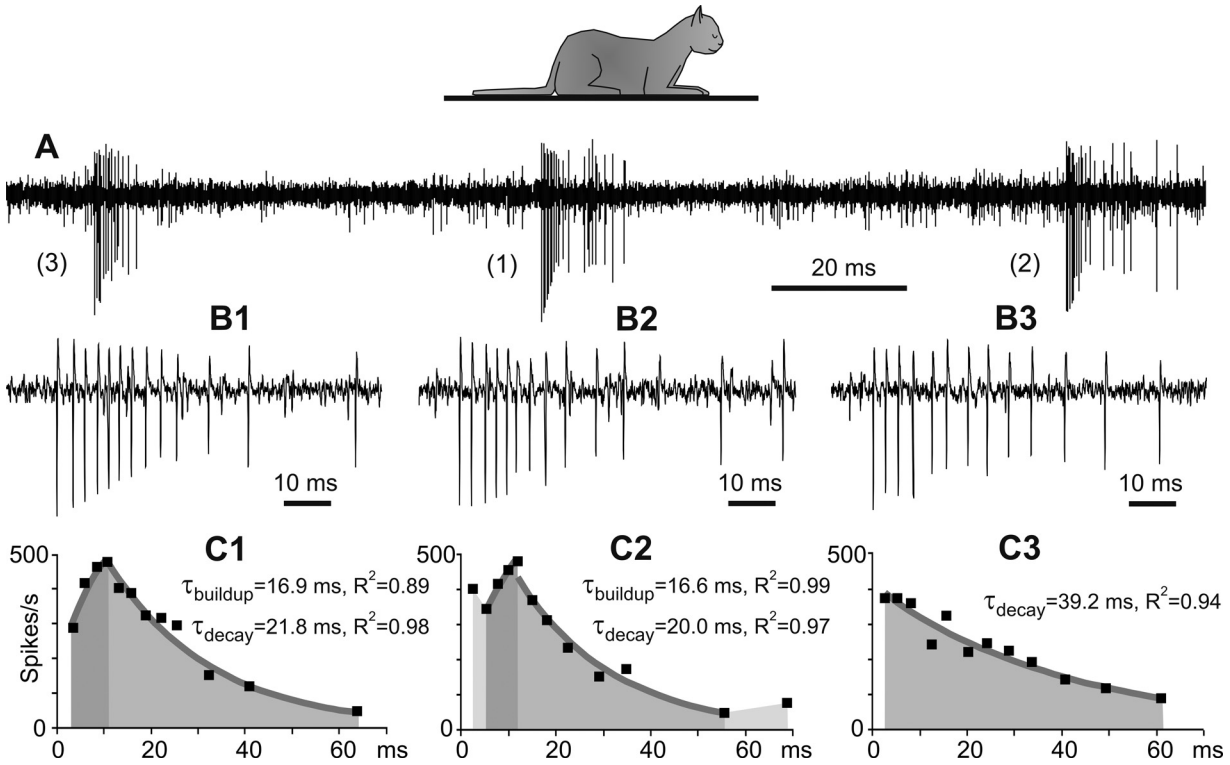

Fig. 2. Variability in the temporal structure of the burst. *A*: fragment of a record from a neuron in the sleeping cat. The neuron spontaneously generated three bursts (*bursts 1*, *2*, and *3*), which differed in the buildup of the firing rate. *B1–B3*: the same bursts shown on an expanded timescale. *C1–C3*: instantaneous firing rates during these bursts (black squares). The buildup and decay of the firing rate are fit with exponents, which are depicted with gray lines. Dark and medium gray areas indicate periods of exponential buildup and decay, respectively. Time constants and determination coefficients of fits are indicated. Changes in the firing rate that preceded and followed exponential buildup and decay are indicated with light gray (*C2*).

firing during both full-scale and atypical bursts had similarly exponential decay (Fig. 2, *C1–C3*).

Of the 1,437 bursts that occurred during sleep, three-quarters (1,094, 76%) were full-scale bursts and one-quarter were atypical bursts (343, 24%) consisting of similar numbers of altered (172, 12%) and short (171, 12%) bursts (Fig. 3*A*).

Bursts during standing are similar to bursts during sleep. More than half of all neurons (35/58, 60.3%) generated bursts of spikes not only while the cats were asleep but also when they were alert and were standing in front of the feeding dish waiting for food. In the sample of 22 neurons that generated bursts in all conditions of our experiment, 670 bursts occurred during standing (Fig. 3*B*). The distribution of the various types of bursts was similar to that found in sleeping cats. Three-quarters of the bursts (492, 73%) were full-scale bursts. The duration and number of spikes composing full-scale bursts during standing (63 ± 19 ms and 12 ± 3 spikes) were similar to those during sleep (Fig. 1, *E* and *I*). One-quarter of bursts were atypical (178, 27%), consisting of similar numbers of altered (80, 12%) and short (98, 15%) bursts.

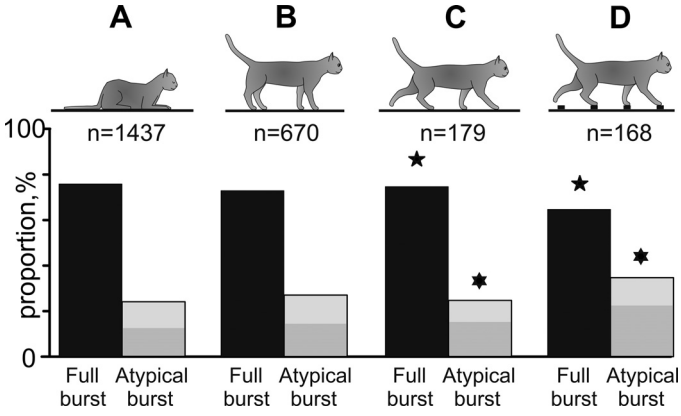

Fig. 3. Proportions of full-scale and atypical bursts during different behaviors. Silhouettes of cats indicate behaviors. Numbers of bursts used for data analyses during each behavior are indicated. Proportions of full-scale bursts are shown as black bars. Proportions of atypical bursts are shown as gray bars (light gray areas represent altered bursts, and dark gray areas show short bursts). Pairs of data that are statistically different ($P < 0.05$, *t*-test) are marked with similar symbols (stars and David stars).

The frequency of burst occurrences varied between neurons with different receptive fields. All but one neuron that responded to stimulation of the paw or wrist (12/13, 92.3%) generated bursts. The probability of burst occurrences in these neurons was 0.8 ± 0.41 bursts/s (Fig. 4*A*). In contrast, only half of the neurons that were responsive to movements in the elbow (3/7, 42.9%) or shoulder (10/18, 55.6%) or did not have receptive fields (10/20, 50%) generated bursts. The probability of burst occurrences in these neurons was half of that seen in wrist/paw-responsive neurons: 0.4 ± 0.12 bursts/s in elbow-related neurons ($P = 0.002$, 2-tailed *t*-test), 0.4 ± 0.33 bursts/s in shoulder-related neurons ($P = 0.004$, 2-tailed *t*-test), and even fewer, 0.2 ± 0.21 bursts/s, in neurons without receptive field ($P < 0.001$, 2-tailed *t*-test) (Fig. 4*A*).

Burst structure during walking depends on complexity of the task. During recording from each neuron, cats walked between 8 and 30 (23 ± 6) times through the corridors. From these trials, 16–78 strides (51 ± 15) during walking on the flat

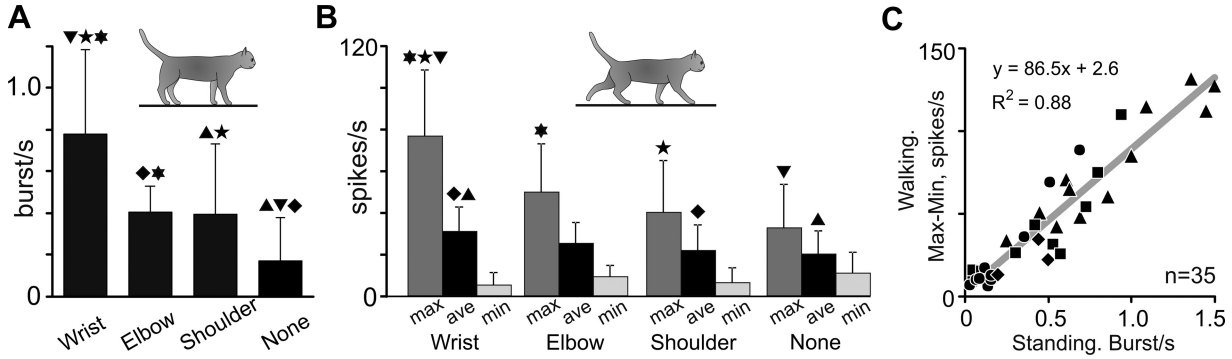

Fig. 4. Modulation of the firing rate during locomotion correlates with the burst probability during standing. *A*: probability of burst occurrence during standing in neurons with different receptive fields. *B*: maximal, average, and minimal firing rates during walking in neurons with different receptive fields. In *A* and *B*, pairs of data different with a confidence of $P < 0.05$ (*t*-test) are indicated with similar symbols (triangles, diamonds, stars, David stars). *C*: in the population of neurons, the magnitude of firing rate modulation (difference between maximal and minimal rates) during walking increased linearly with the probability of burst occurrence during standing. Regression is shown with a gray line; the equation and determination coefficient of the fit are indicated. Neurons related to the wrist or paw are depicted with triangles, neurons responsive to the elbow are shown with diamonds, shoulder-related neurons are represented with squares, and neurons without receptive fields are shown with circles.

surface and along the ladder were chosen for analysis according to the criteria described in METHODS. In the entire sample of neurons, stride duration varied between 660 and 830 ms, which corresponded to a walking speed of 0.6–0.8 m/s. Walking along the ladder was a little slower than on the flat surface, as the average duration of strides on the ladder was 741 ± 32 ms compared with 775 ± 37 ms on the flat surface ($P = 0.03$).

During walking, the firing activity of all neurons was modulated in the rhythm of strides: it increased in one phase of the stride and decreased in another phase. More than a third of neurons (22/58, 37.9%) generated bursts. The firing activity of a representative wrist-related neuron during 34 strides of walking on the flat surface and the ladder is shown in Fig. 5, *A–G*. During both locomotor tasks, this neuron discharged most intensively at the end of the swing phase and the beginning of the stance phase, while being almost inactive in the middle of stance. The spikes identified as belonging to bursts are depicted with color symbols in rasters (Fig. 5, *A* and *B*). Identification of two types of bursts and one nonburst activity is illustrated in Fig. 5, *C–E*. Each of these graphs shows an increased firing activity of the neuron during similar periods of three strides highlighted with a yellow box in Fig. 5*B*. Figure 5*C* shows a spike sequence with orderly changes in the firing rate that were approximated as an exponential buildup followed by an exponential decay; this spike sequence was identified as a full-scale burst. Figure 5*D* shows a spike sequence with orderly changes in the firing rate decay that was approximated with an exponential function; this spike sequence was identified as a short burst. Finally, Fig. 5*E* shows a spike sequence with the irregularly changing firing rate that was not classified as a burst. In Fig. 5, *F* and *G*, the firing rate of the neuron averaged across 34 strides of each locomotor task is shown with a gray area and burst likelihood is shown with a red line. During both tasks, bursts emerged with a similar likelihood of ~0.03 bursts/step, and nearly all occurred at the end of the swing phase. There were differences in the temporal structure of the bursts generated during the two tasks, however. The majority of bursts that occurred during walking on the flat surface were full-scale bursts (5/7, 71%; Fig. 5*A*), which corresponded to their likelihood of 0.15 (5/34) bursts/step. In contrast, during walking on the ladder, the number of full-scale bursts and their likelihood decreased [3/7, 43%; 0.09 (3/34) bursts/step, respectively, Fig. 5*B*], while the proportion and likelihood of atypical bursts, both altered and short, increased from 2/7, 29% [0.06 (2/34)] bursts/step to 4/7, 57% [0.12 (4/34)] bursts/step, respectively.

In the firing activity of neurons we identified 179 bursts during walking on the flat surface and 168 bursts during walking on the ladder. The full-scale bursts recorded during both walking tasks had similar durations and numbers of spikes (65 ± 21 ms and 12 ± 2 spikes; 69 ± 24 ms and 12 ± 2 spikes, respectively) (Fig. 1, *F*, *G*, *J*, and *K*); these parameters were similar to those of the full-scale bursts observed during sleep and standing.

Differences in the temporal structure of bursts during the two locomotor tasks were evident in the whole sample of bursts identified during walking (Table 1). The distribution of types of bursts during walking on the flat surface was similar to those during sleep and standing: three-quarters of these bursts (135/179, 75%) were full-scale bursts, and one-quarter were atypical bursts (44/179, 25%), which consisted of similar numbers of altered (18/179, 10%) and short (26/179, 15%) bursts (Fig. 3*C*). In contrast, during walking on the ladder, the proportion of full-scale bursts was smaller (110/168, 65%, $P = 0.04$, χ^2-test), while the proportion of atypical bursts was larger (58/168, 35%, $P = 0.04$, χ^2-test). Atypical bursts consisted of 14% (23/168) altered and 21% (35/168) short bursts (Fig. 3*D*).

Bursts of different types had different likelihoods of appearance during the stride (Table 1). During walking on the flat surface, the average likelihood of full-scale bursts (0.10 ± 0.09 bursts/step) exceeded significantly the likelihood of atypical bursts (0.03 ± 0.06 bursts/step) ($P = 0.027$, 2-tailed *t*-test) (Fig. 5*H*). In contrast, during walking on the ladder, the likelihood of full-scale bursts was smaller (0.06 ± 0.07 bursts/step), while the likelihood of atypical bursts was larger (0.05 ± 0.06 bursts/step) and almost identical to that of full-scale bursts ($P = 0.207$, 2-tailed *t*-test) (Fig. 5*I*).

Burst occurrences differed between neurons with different receptive fields. The firing behavior of neurons related to the wrist, paw, and shoulder and neurons without receptive fields is illustrated in Fig. 6 with six sets of panels. In each set, the top panel (*index 1*) shows burst likelihood in individual neurons as horizontal red bars of varied saturation; the middle panel (*index 2*) shows the firing rate of the same neurons as horizontal bars of different colors. The lower panel (*index 3*)

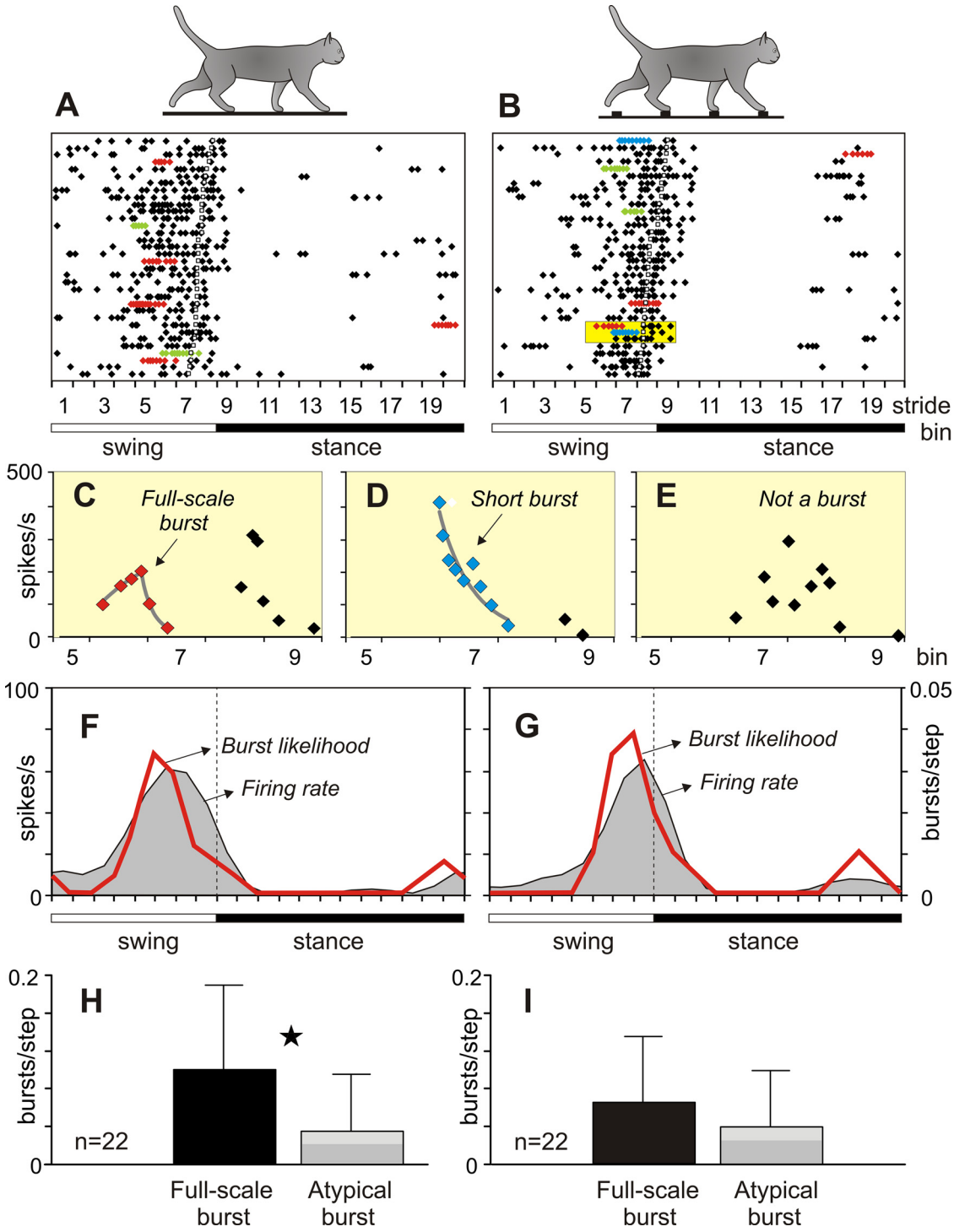

Fig. 5. Burst variability during different locomotor tasks. *A* and *B*: rasters of spikes of a representative neuron during 34 strides of walking on the flat surface (*A*) and on the ladder (*B*). Sequences of spikes identified as bursts are depicted with color symbols: full-scale bursts are red, altered bursts are green, and short bursts are blue. In *B*, a yellow box encloses fragments of an elevated firing activity during 3 strides. *C*: *top* fragment from the yellow box: changes in the firing rate were approximated as an exponential buildup followed by an exponential decay; this spike sequence was identified as a full-scale burst (red symbols). *D*: *middle* fragment from the yellow box: changes in the firing rate were approximated as an exponential decay; this spike sequence was identified as a short burst (blue symbols). *E*: *bottom* fragment from the yellow box: changes in the firing rate were irregular, and the spike sequence was not qualified as a burst. *F* and *G*: average firing rate (gray area) and burst likelihood (red line) of the neuron during walking on the flat surface (*F*) and the ladder (*G*). *Left* *y*-axis represents the firing rate (spikes/s); *right* *y*-axis represents burst likelihood (bursts/step). *H* and *I*: likelihood of bursts of different types during walking on the flat surface (*H*) and the ladder (*I*). Black bars show full-scale bursts; gray bars show atypical bursts: light gray represents altered bursts, and dark gray represents short bursts. The pair of data different with a confidence of $P < 0.05$ (*t*-test) is indicated with a star.

Table 1. *Burst likelihood during locomotion*

Proportion of bursts of different types during locomotion	
Walking on flat surface	179
Full-scale burst	135 (75%)*
Atypical burst	44 (25%)**
Altered burst	18 (10%)
Short burst	26 (15%)
Walking on ladder	168
Full-scale burst	110 (65%)*
Atypical burst	58 (35%)**
Altered burst	23 (14%)
Short burst	35 (21%)
Burst likelihood during step cycle	
Walking on flat surface	0.13 ± 0.16
Full-scale burst	0.10 ± 0.09***
Atypical burst	0.03 ± 0.06***
Walking on ladder	0.11 ± 0.11
Full-scale burst	0.06 ± 0.07
Atypical burst	0.05 ± 0.06

Pairs of categories different with a confidence of $P < 0.05$ are indicated with * and ** (χ^2-test) and *** (*t*-test).

presents the average firing rate (gray area) and average burst likelihood (red line) for the group of neurons. During walking, bursts of spikes occurred most frequently in neurons with receptive fields on the wrist or paw: two-thirds of these neurons (9/13, 69.2%) generated bursts while cats were walking on the flat floor or the ladder (Fig. 6, *A1* and *B1*). Bursts were only half as frequent in shoulder-related neurons (6/18, 33.3%) (Fig. 6, *C1* and *D1*) and neurons without receptive fields (6/20, 30%) (Fig. 6, *E1* and *F1*) and were almost absent in elbow-related neurons (1/7, 14.3%).

The burst likelihood during the two locomotion tasks varied between neurons in a wide range of 0.01–0.6 bursts/step and peaked primarily at the end of the stance phase (Fig. 6, *A3–F3*). The burst likelihood was the highest in wrist/paw-related neurons: 0.2 ± 0.23 bursts/step during walking on the flat surface and 0.17 ± 0.13 bursts/step during walking on the ladder. It had a tendency to be lower in shoulder-related neurons, 0.09 ± 0.07 bursts/step and 0.11 ± 0.07 bursts/step during walking on the flat surface and the ladder, respectively, and was significantly lower in neurons without receptive fields, 0.06 ± 0.05 and 0.04 ± 0.05 bursts/step, respectively ($P <$ 0.05, 2-tailed *t*-test).

Firing rate modulation during locomotion correlates with burst probability during standing. The stride-related modulation of the firing activity of neurons during locomotion correlated with their aptitude for burst generation during standing. During walking on the flat surface, the average firing rate was greatest in neurons responsive to stimulation of the wrist or paw (33 ± 13.2 spikes/s), it tended to be lower in the group of neurons sensitive to movements of the elbow (24.0 ± 3.4 spikes/s) and shoulder (24.8 ± 16.5 spikes/s), and it was smallest in neurons without receptive fields (19.7 ± 11.9 spikes/s, $P = 0.023$, 2-tailed *t*-test) (Fig. 4*B*). Even more conspicuous were differences between wrist/paw-related neurons and other cell groups in respect to their maximal firing rates during the stride. The maximal firing rate in neurons responsive to stimulation of the wrist or paw was 82.7 ± 34.6 spikes/s. It was significantly higher than that of neurons sensitive to elbow movements, 37.2 ± 14.3 spikes/s ($P = 0.007$, 2-tailed *t*-test), neurons sensitive to shoulder movements, 46.2 ± 31.2 spikes/s ($P = 0.017$), and neurons without receptive

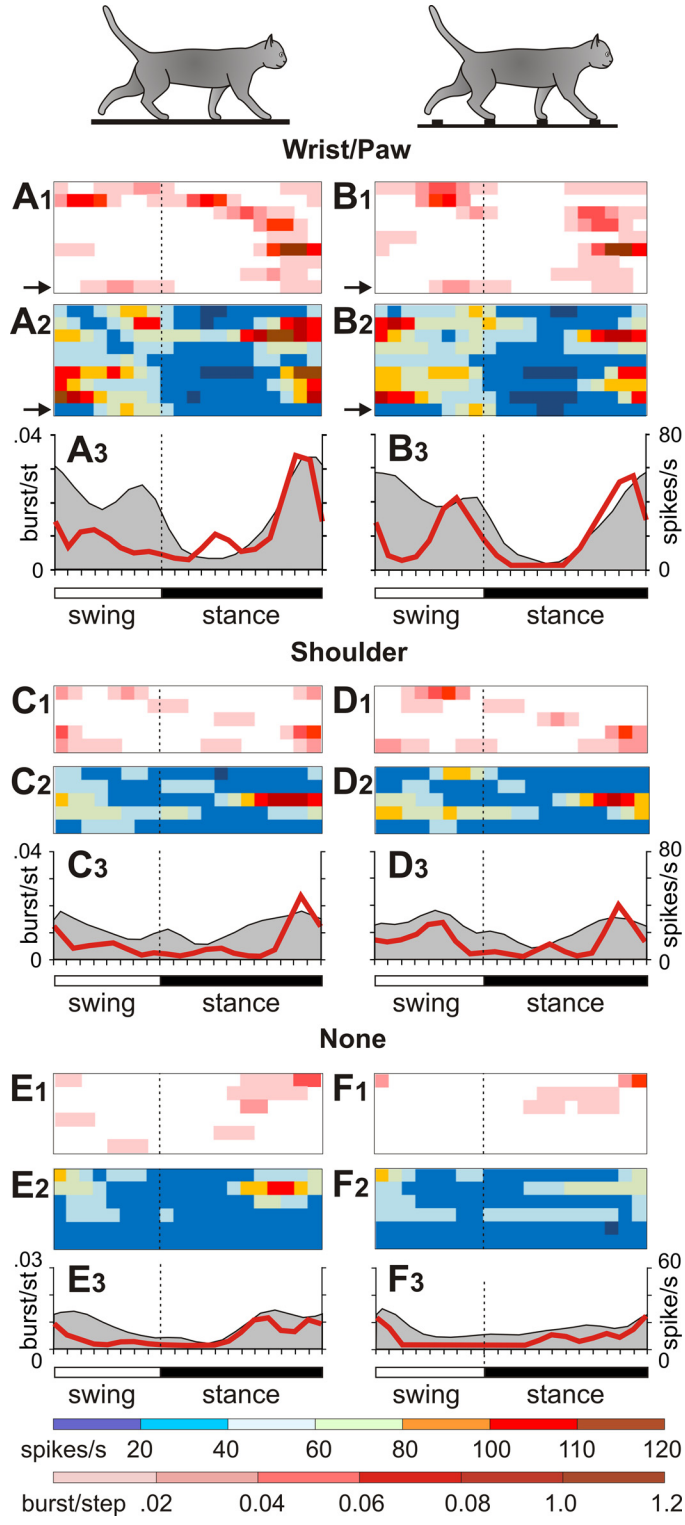

Fig. 6. Burst occurrence in neurons with receptive fields on different segments of the forelimb. *A* and *B*: firing behavior of wrist/paw-related neurons during walking on the flat surface (*A*) and the ladder (*B*). *C* and *D*: firing behavior of shoulder-related neurons. *E* and *F*: firing behavior of neurons without receptive fields. Panels with an *index 1* show the likelihood of bursts during the stride. Panels with an *index 2* show the firing rate during the stride. Each row represents an individual neuron. Burst occurrences and firing rates of the neuron depicted in Fig. 5 are indicated with arrows. The burst likelihood and the firing rate are color-coded according to the scales shown at *bottom*. Panels with an *index 3* show the average firing rate (gray area) and the average burst likelihood (red line) during the stride for the group of neurons.

field, 35.6 ± 27.7 spikes/s (P = 0. 0.002) (Fig. 4*B*). At the same time, minimal firing rates in wrist-, elbow-, and shoulder-related neurons and neurons without receptive fields were similar (Fig. 4*B*). There was a strong relationship between the magnitude of modulation of locomotion-related activity (the difference between the maximal and minimal firing rates during the stride) and the propensity of neurons to generate bursts during standing (Fig. 4*C*). The relationship was linear and could be approximated with a high level of determination as: FR(max − min)= 86.5x + 2.6 (spikes/s), R^2 = 0.88.

DISCUSSION

In this study, we analyzed the firing activity of RE neurons of the cat during four behaviors: sleep, standing, unconstrained walking on a flat surface, and accurate stepping on a horizontal ladder. It is generally accepted that the principal feature of the firing activity of RE neurons is bursts of spikes with a characteristic acceleration-deceleration temporal pattern (e.g., Domich et al. 1986). Previous reports have noted that these bursts may vary in duration, number of spikes, and peak firing rate (Domich et al. 1986; Mukhametov et al. 1979), and bursts starting with the highest firing rate were occasionally observed (e.g., Fig. 5A in Mulle et al. 1986 and Fig. 3 in Contreras et al. 1993). However, the variability in the discharge rate during the initial phase of the burst never drew attention and had not been analyzed. We found that the pattern of spike occurrence during the initial phase of a burst can deviate from the characteristic order, and the amount of deviations increases with the complexity of locomotor behavior. We discriminated bursts from other irregularities in the firing activity by testing how an exponential function fits changes in the instantaneous firing rate during epochs of elevated activity. We found that changes in the firing rate during acceleration and deceleration periods of the characteristic, full-scale burst generated by the RE neuron could be accurately approximated as an exponential buildup and decay. We also found that RE neurons generated atypical bursts, which started with a high firing rate, while their deceleration phase remained unchanged.

We believe that variations in the acceleration period of the burst can be understood when considering the activation of voltage-dependent ion channels in RE neurons. Sodium action potentials generated by RE neurons during the burst result from membrane depolarization caused by broad low-amplitude spikes produced by Ca^{2+} current via T-type channels that open at −70 to −90 mV membrane potential (Avanzini et al. 1989; Bal and McCormick 1993; Coulon et al. 2009; Cueni et al. 2008; Huguenard and Prince 1992; Mulle et al. 1986). The available data suggest that full-scale bursts are generated when the cell's hyperpolarization is maximal, while incomplete bursts are generated at a lower membrane hyperpolarization (Avanzini et al. 1989; Bal and McCormick 1993; Contreras et al. 1993). It is likely that a decrease in the membrane hyperpolarization shortens the rising time of the Ca^{2+} spike and prompts a rapid increase in the firing rate at the very beginning of the burst (Huguenard and Prince 1992). As a result, the buildup of the firing rate deviates from the exponential order. Irrespective of the shape of the acceleration phase of a burst, the maximum in the firing rate was always followed by an exponential decay, which time constant did not significantly vary. This decay reflects the kinetics of Ca^{2+} current inactivation, which is voltage independent and has a long (80–100 ms) time constant (Avanzini et al. 1989; Huguenard and Prince 1992; Mulle et al. 1986).

Neurons in the RE and relay thalamic nuclei generate bursts not only during sleep but also during wakefulness (Domich et al. 1986; Fanselow et al. 2001; Guido and Weyand 1995; Marlinski et al. 2012b; Weyand et al. 2001). In our study, bursts were seen in half of the neurons when cats were standing in front of the feeding dish waiting for food to be dispensed and in a third of the neurons during both unconstrained walking and accurate stepping on the ladder. Importantly, probability of bursts during standing was predictive of a neuron's locomotion-related discharge frequency modulation (Fig. 4*C*), suggesting that both types of firing activity are substantially influenced by intrinsic spike discharge properties of RE neurons. As we reported previously, the occurrence of bursts during locomotion was frequently aligned with the beginning of the period of elevated firing activity during the stride (Marlinski et al. 2012b). Typically, preferred phases of locomotor-related increases in the firing activity of RE neurons during walking on the flat surface and the ladder were similar. Correspondingly, the timing of bursts as well as their likelihood did not vary significantly between the two locomotor tasks (Fig. 6). However, the temporal pattern of spikes during the burst did depend on the complexity of the locomotor task. During walking on the flat surface the likelihood of full-scale bursts was significantly higher than that of atypical bursts, but during walking on the ladder atypical bursts occurred as often as full-scale bursts (Fig. 5, *H* and *I*). This effect may indicate that during walking on the ladder the RE neurons were less hyperpolarized than during walking on the flat surface (see, e.g., Fig. 3 in Contreras et al. 1993). Such a decrease in hyperpolarization could result from an enhancement in excitatory inputs from the VL and motor cortex related to an increase in the complexity of the locomotor task. We have previously shown that stride-related modulation of the firing activity in numerous neurons in both the VL and layer VI of the motor cortex was more profound during walking along a horizontal ladder compared with that during walking on a flat surface (Marlinski et al. 2012a; Sirota et al. 2005).

The firing behavior of RE neurons reflects the combined processing of signals from their two principal inputs, thalamic and cortical. The result of this processing depends on two factors: synaptic connections between thalamo-reticular and cortico-reticular fibers and RE neurons and the activity of thalamic and cortical cells from which these fibers originate. It appears that the thalamo-reticular input has more potential for shaping the firing behavior of RE neurons than the cortico-reticular input. Indeed, thalamo-reticular terminals are more frequent on the soma and proximal dendrites, while cortico-reticular terminals are primarily located on the distal dendrites (Liu and Jones 1999; Montero 1989). In addition, although thalamo-reticular synapses are less numerous than cortico-reticular synapses, the efficacy of signal transmission in thalamo-reticular synapses is higher than in cortico-reticular synapses (Gentet and Ulrich 2003, 2004; Liu and Jones 1999; Liu et al. 2001). In our experiments, we found similarity in bursts generated by RE neurons when cats slept, stood, or walked on the flat surface, all of which are behaviors that do not require participation of the thalamo-cortical circuits (Beloozerova and Sirota 1993; Chambers and Liu 1957; Friel et al.

2007; Liddell and Phillips 1944; Metz and Whishaw 2002; Trendelenburg 1911). During these three behaviors, RE neurons usually generated full-scale bursts of spikes. The temporal structure of bursts was altered: full-scale bursts became less frequent and the proportion of atypical bursts increased when cats walked on the horizontal ladder, which was a complex locomotor task that required participation of the motor cortex. It is likely that the firing activity of the motor cortex neurons associated with the motor command for accurate stepping on the ladder's crosspieces was ultimately transferred to the RE. As a result, the firing behavior of RE neurons during complex locomotion was affected by signals from their cortical inputs added to signals from thalamic inputs. Convergence of ascending and descending pathways was proposed to be a critical element for determination of the firing mode of thalamic relay nuclei neurons that modify transmission of somatosensory signals (Nicolelis and Fanselow 2002). It is likely that the same is true for neurons in the RE. As indicated above, in these neurons, in contrast to full-scale bursts with an initial gradual increase in the firing rate, atypical bursts began with a high rate of firing. Thus, during complex locomotion, the inhibitory postsynaptic responses of VL neurons to their RE inputs could be potentiated when elicited by bursts of spikes that follow each other with high frequency from the beginning. We suggest that these changes in the temporal pattern of burst of inhibitory RE neurons could facilitate the tuning of thalamo-cortical signals to the complexity of an ongoing behavioral task. It was previously shown that in domains of other modalities RE activity modifies neuronal discharges in the thalamic nucleus from which it receives its input (Cotillon-Williams et al. 2008; Funke and Eysel 1998; Temereanca and Simons 2004). An accurate understanding of how this tuning influences locomotor kinematics can be achieved in the future with simultaneous recordings of RE neuron activities and limb movement mechanics. At present, we can outline only a general scheme of the relationship between the firing of neurons in the motor section of the RE and forebrain control of different segments of the forelimb during locomotion.

In our previous study, we found profound differences between the locomotion-related firing behavior of RE neurons with receptive fields on the distal and proximal forelimb (Marlinski et al. 2012b). The average firing rate and the magnitude of the firing rate modulation, which determines the intensity of the inhibitory reticulo-thalamic signaling, were distinctively higher in wrist/paw-related neurons compared with shoulder-related neurons. Concurrently, the probability of burst occurrence during standing and the likelihood of bursts during locomotion were the highest in wrist/paw-related neurons. Distinctions between wrist/paw- and shoulder-related neurons could be seen as a manifestation of the existence of two classes of RE neurons, which differ in their ability to generate bursts and in responsiveness to transsynaptic inputs (Brunton and Charpak 1997; Contreras et al. 1992). Significantly, in rat thalamic slices, neurons of these two classes were found to be separated in the RE: neurons discharging bursts are concentrated mostly in the ventral areas while neurons with preferentially tonic firing activity are located in the dorsal areas of the nucleus (Lee et al. 2007). We reported earlier that neurons with receptive fields on the wrist/paw were located ventrally in the nucleus, while neurons with receptive fields on the shoulder were located dorsally in the nucleus (Marlinski et al. 2012b). Taken together, these data point to strategic differences in the thalamo-cortical processing of signals related to movements of proximal and distal parts of the forelimb (Fig. 7). Commands controlling movements of the proximal limb moderately activate inhibitory RE neurons. As a result, ascending signals related to movements of the proximal limb can reach the motor cortex without significant attenuation at any time during the stride. This could support continuous context-related modification of the activity of the cortical neurons that control movements of the proximal limb. In contrast, the commands controlling movements of the distal forelimb significantly enhance the activity of inhibitory RE neurons. During locomotion, an augmentation of the inhibitory reticulo-thalamic activity is primarily tuned to the particular phase of the stride: the end of the stance. This phase is critical for planning of the trajectory of the forthcoming step in a complex environment (Hollands and Marple-Horvat 1996; Laurent and Thomson 1988). An increase in the activity of inhibitory RE neurons elicited by this motor command would attenuate ongoing thalamo-cortical signals. As a result, only strong ascending signals relevant for adaptation of the forthcoming movement of the distal forelimb could reach the cortex and modify the motor command during this period of the stride. We have shown previously that both motor cortex and VL neurons with receptive fields on the proximal and distal parts of the forelimb have different firing behavior during unconstrained walking as well as accurate stepping (Marlinski et al. 2012a; Stout and Beloozerova 2012). Thus the motor cortex, motor thalamus, and motor sector of the RE work in concert to optimize movements of different segments of the limbs that enable locomotion in environments of varying complexities.

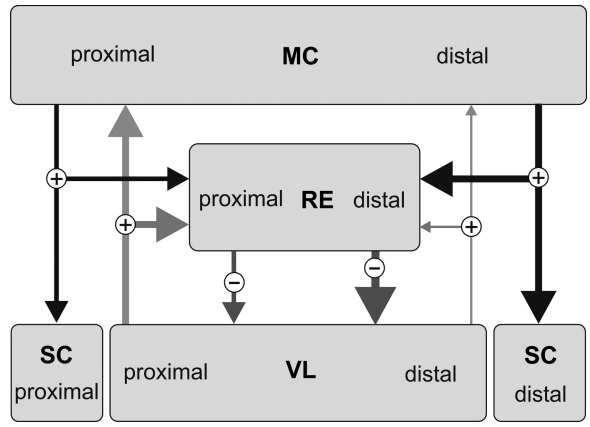

Fig. 7. The motor sector of the RE gates differently thalamo-cortical signals related to the distal and proximal forelimb. Arrow width indicates hypothesized efficacy of connections. Circled plus and minus signs indicate excitatory and inhibitory inputs, respectively. MC, motor cortex; SC, spinal cord; VL, ventrolateral nucleus of the thalamus. "Proximal" and "distal" indicate compartments of neural structures related to corresponding parts of the forelimb. See text for detailed explanation.

ACKNOWLEDGMENTS

The authors are grateful to Peter Wettenstein for exceptional engineering support, Megan Foe and Qasim Rahman for assistance with data analysis, and Dr. Thomas Hamm for valuable comments on the data presentation.

GRANTS

This research was supported by National Institute of Neurological Disorders and Stroke Grant R01 NS-058659 to I. N. Beloozerova.

DISCLOSURES

No conflicts of interest, financial or otherwise, are declared by the author(s).

AUTHOR CONTRIBUTIONS

Author contributions: V.M. and I.N.B. conception and design of research; V.M. and I.N.B. performed experiments; V.M. analyzed data; V.M. and I.N.B. interpreted results of experiments; V.M. prepared figures; V.M. drafted manuscript; V.M. and I.N.B. edited and revised manuscript; V.M. and I.N.B. approved final version of manuscript.

REFERENCES

Arcelli P, Frassoni C, Regondi MC, De Biasi S, Spreafico R. GABAergic neurons in mammalian thalamus: a marker of thalamic complexity? *Brain Res Bull* 42: 27–37, 1997.

Avanzini G, de Curtis M, Panzica F, Spreafico R. Intrinsic properties of nucleus reticularis thalami neurones of the rat studied in vitro. *J Physiol* 416: 111–122, 1989.

Bal T, McCormick DA. Mechanisms of oscillatory activity in guinea-pig nucleus reticularis thalami in vitro: a mammalian pacemaker. *J Physiol* 468: 669–691, 1993.

Beloozerova IN, Farrell BJ, Sirota MG, Prilutsky BI. Differences in movement mechanics, electromyographic, and motor cortex activity between accurate and nonaccurate stepping. *J Neurophysiol* 103: 2285–2300, 2010.

Beloozerova IN, Sirota MG. The role of the motor cortex in the control of accuracy of locomotor movements in the cat. *J Physiol* 461: 1–25, 1993.

Beloozerova IN, Sirota MG. Integration of motor and visual information in the parietal area 5 during locomotion. *J Neurophysiol* 90: 961–971, 2003.

Bishop PO, Burke W, Davis R. The identification of single units in central visual pathways. *J Physiol* 162: 409–431, 1962.

Brunton J, Charpak S. Heterogeneity of cell firing properties and opioid sensitivity in the thalamic reticular nucleus. *Neuroscience* 78: 303–307, 1997.

Carman JB, Cowan WM, Powell TP. Cortical connections of the thalamic reticular nucleus. *J Anat* 98: 587–598, 1964.

Chambers WW, Liu CN. Corticospinal tract of the cat: an attempt to correlate the pattern of degeneration with deficits in reflex activity following neocortical lesions. *J Comp Neurol* 108: 23–55, 1957.

Contreras D, Curró Dossi R, Steriade M. Bursting and tonic discharges in two classes of reticular thalamic neurons. *J Neurophysiol* 68: 973–977, 1992.

Contreras D, Curró Dossi R, Steriade M. Electrophysiological properties of cat reticular thalamic neurones in vivo. *J Physiol* 470: 273–294, 1993.

Cotillon-Williams N, Huetz C, Hennevin E, Edeline JM. Tonotopic control of auditory thalamus frequency tuning by reticular thalamic neurons. *J Neurophysiol* 99: 1137–1151, 2008.

Coulon P, Herr D, Kanyshkova T, Meuth P, Budde T, Pape HC. Burst discharges in neurons of the thalamic reticular nucleus are shaped by calcium-induced calcium release. *Cell Calcium* 46: 333–346, 2009.

Crabtree JW. The somatotopic organization within the cat's thalamic reticular nucleus. *Eur J Neurosci* 4: 1352–1361, 1992.

Cueni L, Canepari M, Luján R, Emmenegger Y, Watanabe M, Bond CT, Franken P, Adelman JP, Lüthi A. T-type Ca^{2+} channels, SK2 channels and SERCAs gate sleep-related oscillations in thalamic dendrites. *Nat Neurosci* 11: 683–692, 2008.

Domich L, Oakson G, Steriade M. Thalamic burst patterns in the naturally sleeping cat: a comparison between cortically projecting and reticularis neurones. *J Physiol* 379: 429–449, 1986.

Fanselow EE, Sameshima K, Baccala LA, Nicolelis MA. Thalamic bursting in rats during different awake behavioral states. *Proc Natl Acad Sci USA* 98: 15330–15335, 2001.

Friel KM, Drew T, Martin JH. Differential activity-dependent development of corticospinal control of movement and final limb position during visually guided locomotion. *J Neurophysiol* 97: 3396–3406, 2007.

Fuller JH, Schlag JD. Determination of antidromic excitation by the collision test: problems of interpretation. *Brain Res* 112: 283–298, 1976.

Funke K, Eysel UT. Inverse correlation of firing patterns of single topographically matched perigeniculate neurons and cat dorsal lateral geniculate relay cells. *Vis Neurosci* 15: 711–729, 1998.

Gentet LJ, Ulrich D. Strong, reliable and precise synaptic connections between thalamic relay cells and neurones of the nucleus reticularis in juvenile rats. *J Physiol* 546: 801–811, 2003.

Gentet LJ, Ulrich D. Electrophysiological characterization of synaptic connections between layer VI cortical cells and neurons of the nucleus reticularis thalami in juvenile rats. *Eur J Neurosci* 19: 625–633, 2004.

Govindaiah G, Cox CL. Metabotropic glutamate receptors differentially regulate GABAergic inhibition in thalamus. *J Neurosci* 26: 13443–14353, 2006.

Guido W, Weyand T. Burst responses in thalamic relay cells of the awake behaving cat. *J Neurophysiol* 74: 1782–1786, 1995.

Guillery RW, Harting JK. Structure and connections of the thalamic reticular nucleus: advancing views over half a century. *J Comp Neurol* 463: 360–371, 2003.

Hartings JA, Temereanca S, Simons DJ. State-dependent processing of sensory stimuli by thalamic reticular neurons. *J Neurosci* 23: 5264–5271, 2003.

Hollands MA, Marple-Horvat DE. Visually guided stepping under conditions of step cycle-related denial of visual information. *Exp Brain Res* 109: 343–356, 1996.

Houser CR, Vaughn JE, Barber RP, Roberts E. GABA neurons are the major cell type of the nucleus reticularis thalami. *Brain Res* 200: 341–354, 1980.

Huguenard JR, Prince DA. A novel T-type current underlies prolonged Ca^{2+}-dependent burst firing in GABAergic neurons of rat thalamic reticular nucleus. *J Neurosci* 12: 3804–3817, 1992.

Jones EG. Some aspects of the organization of the thalamic reticular complex. *J Comp Neurol* 162: 285–308, 1975.

Lam YW, Sherman SM. Different topography of the reticulothalmic inputs to first- and higher-order somatosensory thalamic relays revealed using photostimulation. *J Neurophysiol* 98: 2903–2909, 2007.

Lam YW, Sherman SM. Functional organization of the thalamic input to the thalamic reticular nucleus. *J Neurosci* 31: 6791–6799, 2011.

Laurent M, Thomson JA. The role of visual information in control of a constrained locomotor task. *J Mot Behav* 20: 17–37, 1988.

Lee SH, Govindaiah G, Cox CL. Heterogeneity of firing properties among rat thalamic reticular nucleus neurons. *J Physiol* 582: 195–208, 2007.

Liddell EG, Phillips CG. Pyramidal section in the cat. *Brain* 67: 1–9, 1944.

Liu XB, Bolea S, Golshani P, Jones EG. Differentiation of corticothalamic and collateral thalamocortical synapses on mouse reticular nucleus neurons by EPSC amplitude and AMPA receptor subunit composition. *Thalamus Relat Syst* 1: 15–29, 2001.

Liu XB, Jones EG. Predominance of corticothalamic synaptic inputs to thalamic reticular nucleus neurons in the rat. *J Comp Neurol* 414: 67–79, 1999.

Liu XB, Warren RA, Jones EG. Synaptic distribution of afferents from reticular nucleus in ventroposterior nucleus of cat thalamus. *J Comp Neurol* 352: 187–202, 1995.

Marigold DS, Patla AE. Visual information from the lower visual field is important for walking across multi-surface terrain. *Exp Brain Res* 188: 23–31, 2008.

Marlinski V, Beloozerova IN. Burst firing of thalamic reticular nucleus neurons during locomotion (Abstract). *2013 Neuroscience Meeting Planner*. San Diego, CA: Society for Neuroscience, 2013, Program No. 749.21 [Online].

Marlinski V, Nilaweera WU, Zelenin PV, Sirota MG, Beloozerova IN. Signals from the ventrolateral thalamus to the motor cortex during locomotion. *J Neurophysiol* 107: 455–472, 2012a.

Marlinski V, Sirota MG, Beloozerova IN. Differential gating of thalamocortical signals by reticular nucleus of thalamus during locomotion. *J Neurosci* 32: 15823–15836, 2012b.

Metz GA, Whishaw IQ. Cortical and subcortical lesions impair skilled walking in the ladder rung walking test: a new task to evaluate fore- and hindlimb stepping, placing, and co-ordination. *J Neurosci Methods* 115: 169–179, 2002.

Montero VM. Ultrastructural identification of synaptic terminals from cortical axons and from collateral axons of geniculo-cortical relay cells in the perigeniculate nucleus of the cat. *Exp Brain Res* 75: 65–72, 1989.

Mukhametov LM, Rizzolatti G, Tradardi V. Spontaneous activity of neurones of nucleus reticularis thalami in freely moving cats. *J Physiol* 210: 651–667, 1970.

Mulle C, Madariaga A, Deschênes M. Morphology and electrophysiological properties of reticularis thalami neurons in cat: in vivo study of a thalamic pacemaker. *J Neurosci* 6: 2134–2145, 1986.

Nicolelis MA, Fanselow EE. Thalamocortical optimization of tactile processing according to behavioral state. *Nat Neurosci* 5: 517–523, 2002.

Pinault D. The thalamic reticular nucleus: structure, function and concept. *Brain Res Brain Res Rev* 46: 1–31, 2004.

Pinault D, Deschênes M. Projection and innervation patterns of individual thalamic reticular axons in the thalamus of the adult rat: a three-dimensional, graphic, and morphometric analysis. *J Comp Neurol* 391: 180–203, 1998.

Prilutsky BI, Sirota MG, Gregor RJ, Beloozerova IN. Quantification of motor cortex activity and full-body biomechanics during unconstrained locomotion. *J Neurophysiol* 94: 2959–2969, 2005.

Reinagel P, Godwin D, Sherman SM, Koch C. Encoding of visual information by LGN bursts. *J Neurophysiol* 81: 2558–2569, 1999.

Reinoso-Suarez F. *Topographischer Hirnatlas der Katze für experimental-physiologische Untersuchungen*. Darmstadt, Germany: E. Merck, 1961.

Rinvik E. The corticothalamic projection from the pericruciate and coronal gyri in the cat. An experimental study with silver-impregnation methods. *Brain Res* 10: 79–119, 1968.

Rivers TJ, Shah NA, Sirota MG, Beloozerova IN. Where cats look during locomotion with accurate stepping. *2011 Neuroscience Meeting Planner*. Washington, DC: Society for Neuroscience, 2011, Program No. 379.15 [Online].

Scheibel ME, Scheibel AB. The organization of the nucleus reticularis thalami: a Golgi study. *Brain Res* 1: 43–62, 1966.

Sherk H, Fowler GA. Neural analysis of visual information during locomotion. *Prog Brain Res* 134: 247–264, 2001.

Sirota MG, Swadlow HA, Beloozerova IN. Three channels of corticothalamic communication during locomotion. *J Neurosci* 25: 5915–5925, 2005.

Steriade M, Domich L, Oakson G. Reticularis thalami neurons revisited: activity changes during shifts in states of vigilance. *J Neurosci* 6: 68–81, 1986.

Stout EE, Beloozerova IN. Pyramidal tract neurons receptive to different forelimb joints act differently during locomotion. *J Neurophysiol* 107: 1890–1903, 2012.

Swadlow HA, Bezdudnaya T, Gusev AG. Spike timing and synaptic dynamics at the awake thalamocortical synapse. *Prog Brain Res* 149: 91–105, 2005.

Swadlow HA, Gusev AG. The impact of "bursting" thalamic impulses at a neocortical synapse. *Nat Neurosci* 4: 402–408, 2001.

Temereanca S, Simons DJ. Functional topography of corticothalamic feedback enhances thalamic spatial response tuning in the somatosensory whisker/barrel system. *Neuron* 41: 639–651, 2004.

Trendelenburg W. Untersuchungen über reizlose vorübergehende Aussaltung am Zentralnervensystem. III. Die extermitaten Region der Grosshirninde. *Pflügers Arch* 137: 515–544, 1911.

Velayos JL, Jiménez-Castellanos J Jr, Reinoso-Suárez F. Topographical organization of the projections from the reticular thalamic nucleus to the intralaminar and medial thalamic nuclei in the cat. *J Comp Neurol* 279: 457–469, 1989.

Weyand TG, Boudreaux M, Guido W. Burst and tonic response modes in thalamic neurons during sleep and wakefulness. *J Neurophysiol* 85: 1107–1118, 2001.

Yen CT, Conley M, Hendry SH, Jones EG. The morphology of physiologically identified GABAergic neurons in the somatic sensory part of the thalamic reticular nucleus in the cat. *J Neurosci* 5: 2254–2268, 1985.